Atmospheric Environment 74 (2013) 37–44

Contents lists available at SciVerse ScienceDirect

Atmospheric Environment

journal homepage: www.elsevier.com/locate/atmosenv

Measurements of vertical and horizontal distributions of ozone over Beijing from 2007 to 2010

Pengfei Chen [a,b], Jiannong Quan [a,c,*], Qiang Zhang [a,c], Xuexi Tie [d,e,**], Yang Gao [a,c], Xia Li [a,c], Mengyu Huang [a,c]

[a] Beijing Weather Modification Office, Beijing, China
[b] Institue of Urban Meteorology, CMA, Beijing, China
[c] Beijing Key Laboratory of Cloud, Precipitation and Atmospheric Water Resources, Beijing, China
[d] Key Laboratory of Aerosol, SKLLQG, Institute of Earth Environment, Chinese Academy of Sciences, Xian, China
[e] National Center for Atmospheric Research, Boulder, USA

HIGHLIGHTS

- The vertical and horizontal distributions of O_3 over Beijing region was analyzed.
- A peak O_3 concentration occurring at ~1 km over Beijing is observed.
- O_3 concentration in the downwind of the city plumes was enhanced.
- A transition of O_3 formation from VOC-limited to NOx-limited at ~1 km is found.

ARTICLE INFO

Article history:
Received 19 November 2012
Received in revised form
5 March 2013
Accepted 13 March 2013

Keywords:
Ozone
Vertical profile
Horizontal profile
Aircraft measurement
Beijing

ABSTRACT

The vertical distributions of ozone (O_3) over a mega city (Beijing, China), and the horizontal O_3 distributions in the lower troposphere (2–3.6 km) over Beijing and its surrounding areas located in the North China Plain (NCP), were analyzed based on the aircraft measurements from 159 flights during 2007–2010. The results are highlighted as follows: (1) There was a peak of O_3 concentration occurring at ~1 km over Beijing, and the peak values ranged between 60 and 120 ppbv. (2) There was an O_3 minimum at the surface. The minimum was largely caused by the chemical reaction of NO + O_3. This process produced about 30 ppbv of the O_3 reduction below 0.5 km in the morning (9:00–10:00). (3) There was a transition altitude (~1 km), below which the ozone formation was in a VOC-limited condition, and above which the ozone formation was in a NOx-limited condition. (4) The analysis of the horizontal distribution shows that O_3 concentrations were enhanced in the downwind of the city plumes. This result suggests that there was an important regional O_3 chemical production in the NCP region.

1. Introduction

Ozone is a critical trace gas in the troposphere because it plays important roles in atmospheric chemistry, air quality, and climate change (Bojkov, 1988; Akimoto, 2003). The O_3 formation is significantly affected by several important chemical precursors, including volatile organic compounds (VOC) and oxides of nitrogen (NOx) (Sillman, 1995), meteorological factors (Benjamin and Winer, 1998; Tie et al., 2009a), and atmospheric aerosols (Tie et al., 2005).

China's rapid economic growth in recent years has resulted in large increases in pollutant emissions (Ohara et al., 2007; Zhang et al., 2007; Tang et al., 2009; Yang et al., 2011). The NCP region is located in central of China, and the region includes several large cities, such as the mega city of Beijing. The region is one of the most populated and industrialized regions in China and is suffered from the impacts of air pollution in many aspects (Hao and Wang, 2005; Shao et al., 2006; Quan et al., 2011). The O_3 problem is among the most stubborn environmental issues. For example, the concentration of O_3 has frequently exceeded the national air quality standard (Lu et al., 2010; Wang et al., 2009), with a peak hourly averaged concentration of 286 ppbv (Wang et al., 2006). Previous studies focused mainly on the spatial and temporal variations of the surface ozone and its precursors in the NCP region. Several observation data indicated that the surface O_3 concentration in suburb was higher than that in urban over NCP (e.g. Wang et al., 2006; Xu et al., 2011). The analysis of relationship between the rate of

* Corresponding author. Beijing Weather Modification Office, Beijing, China.
** Corresponding author. National Center for Atmospheric Research, Boulder, USA.
E-mail addresses: quanjn1975@gmail.com (J. Quan), xxtie@ucar.edu (X. Tie).

1352-2310/$ – see front matter © 2013 Elsevier Ltd. All rights reserved.
http://dx.doi.org/10.1016/j.atmosenv.2013.03.026

photochemical ozone production (P[O_3]) and it's precursors (NOx and VOCs) indicated that O_3 production in concentrated urban plumes is often in a VOC-limited regime (Shao et al., 2009; An, 2006; Duan et al., 2008; Xu et al., 2011; Lu et al., 2010; Tang et al., 2010). As a result, the high NOx concentration in NCP lead to a strong inhibitory effect on O_3 formation, and the reduction of NOx emissions might produce in accelerating ozone production (Wang et al., 2009; Yang et al., 2011). In addition, the aerosol loadings are extremely heavy in the NCP region (Tie and Cao, 2009), and the heavy loading of aerosols over the NCP region also affects the O_3 formation by reducing solar radiation (Bian et al., 2007a; Han et al., 2009). However, there were only the surface measurements of ozone and its precursors, which were available and used in the previous studies. It is lack of O_3 vertical measurements in the troposphere in NCP. Although satellite and ozonesonde can give some insights of the vertical structure of ozone (Bian et al., 2007b; Wang et al., 2012), the low spatial and temporal resolutions of the above data cannot provide the details of O_3 formation and transport in the lower troposphere.

In this paper, we show the in-situ aircraft measurements of O_3 and its important precursor (NOx) in the NCP region. The time resolution of the measurements is 1 s and the vertical resolution is several decameters. The analysis focuses on the following issues: (a) the vertical distribution of O_3 in the lower troposphere over Beijing; (b) the effect of NOx concentrations on O_3 formation over Beijing; and (c) the horizontal distribution O_3 in the lower troposphere over the NCP region.

2. Description of the measurement

2.1. Instruments on the aircraft

Several commercial instruments were mounted on the aircraft (Y-12) to measure the concentrations of O_3, NOx (NO + NO_2), and other atmospheric pollutants. Ozone was measured using a commercial UV photometric analyzer (Model 49iTL, TEI Inc.). The time resolution was set to 1 s during the aircraft measurement in order to get more spatial information, which might affect the detectable limit of the measurements. For example, the detectable limit decreases from 0.05 ppbv to 0.5 ppbv when the time resolution increases from 120 s to 1 s. The measured O_3 concentrations range from 0.5 to 200 ppbv, with temperature and pressure correction. NO–NO_2–NOx was measured with a chemiluminescent trace level analyzer (Model 42iTL, TEI Inc.). The analyzer has a detection limit of 0.025 ppbv. These analyzers were calibrated before the field campaigns by injecting a span gas mixture in scrubbed ambient air generated by a TEI model 111. The zero check was also conducted. The inlet system was placed in front of the aircraft to avoid the influence of the aircraft exhausts for measurements. Aerosol particles were measured by a passive cavity aerosol spectrometer probe (PCASP-200, DMT Inc.), with the particle size ranging from 0.10 to 3.0 μm in diameter. The meteorological measurements included location, temperature, relative humidity, barometric pressure and wind using an aircraft integrated meteorological measurement system (AIMMS-20, Advantech Research Inc.). The PCASP-200 and AIMMS-20 instruments were amounted under the wing of aircraft.

2.2. Flight information and data process

Fig. 1 displays the horizontal flight routes during 2007–2010. Three airports were used during the experiments, including Shahe (SH), Zhangjiakou (ZJK), and Dingxing (DX) airports. The geographical locations (latitude and longitude) of the three airports are indicated in Fig. 1. The three airports are not for commercial use, and there are only several flights in each day. The effect of the emissions of airplanes is very small, and the measured vertical distributions of gaseous pollutants were insignificantly perturbed by the aircraft emissions. The detailed information for measuring O_3 vertical profiles is described as follows:

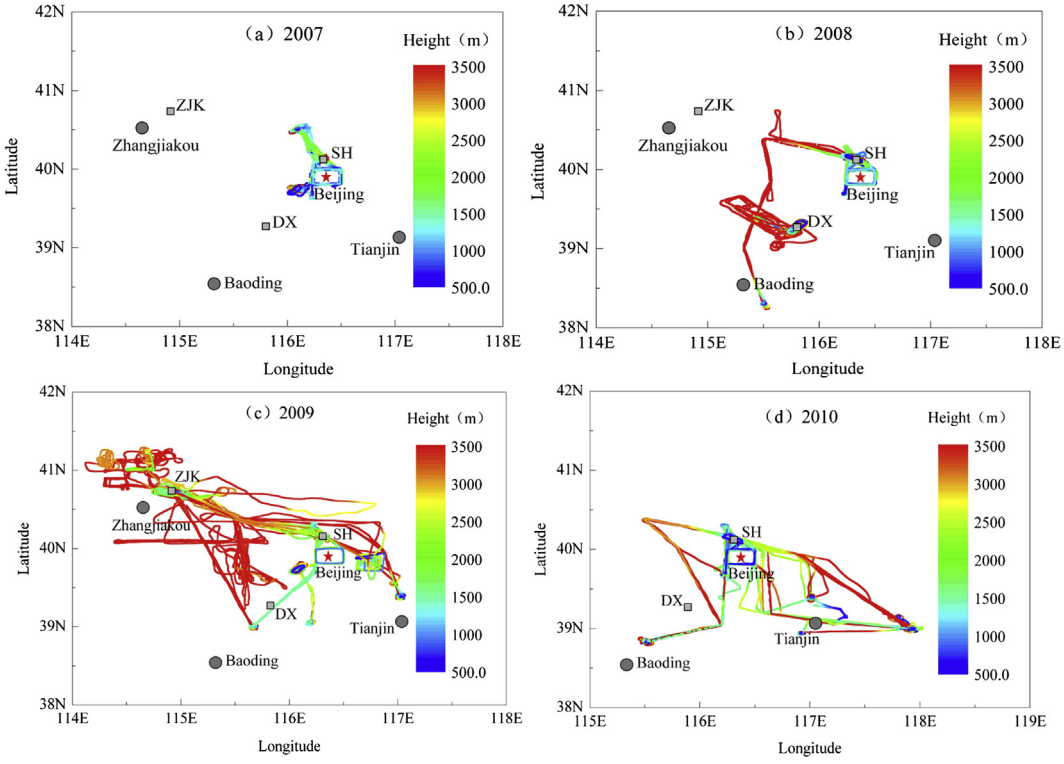

Fig. 1. The horizontal flight routes over NCP during 2007–2010.

Table 1
The flight information between 2007 and 2010.

Year	Apr	May	Jun	Jul	Aug	Sept	Oct	Nov	Total
2007	7	6	17	8	28	15	–	14	95
2008	14	20	8	5	3	–	12	8	70
2009	6	4	8	6	–	–	–	–	24
2010	5	3	7	5	3	–	2	3	28
Total	32	33	40	24	34	15	14	25	217

(i) The aircraft was spiraled down over the airport to measure the vertical profiles before it landed. The flight diameter of the circles was about 10 km, and the upper altitude of these descending vertical profiles was 3.6 m. The descend speed was generally 150 m min^{-1}.
(ii) The data was excluded during overcast days and precipitation conditions, when the solar radiation was significantly reduced and the atmospheric photochemical activity was low.
(iii) The vertical profiles were calculated with a 50 m interval in altitudes, and the statistical outliers were eliminated. We used the criteria of $|C-C_{avg}| > 3SD$ to define the statistical outliers at each specific altitude level, where C_{avg} is of mean concentration of O_3/NOx at a specific altitude level, and SD refers to the standard deviation.
(iv) The horizontal distributions were averaged at 0.05° resolution in the lower troposphere (2–3.6 km). During horizontal detection, the aircraft fly at altitudes ranging from 2 to 3.6 km over the NCP region with a speed of 200–260 km h^{-1}.

As a result, 217 vertical profiles were selected from the original records of 159 flights resulting from the above procedures (Table 1).

3. Analysis of the results

3.1. The spatial and temporal O_3 distributions over NCP

The vertical distribution of O_3 is influenced by local chemistry production, the dynamical processes in the troposphere (Hübler et al., 1998; Mcnider et al., 1998), and the vertical downward transport of ozone from the stratosphere (Warneck, 1988). Fig. 2 shows the monthly averaged O_3 profile from April to November based on 4 year (2007–2010) aircraft measurements. The variation of ozone with altitude was remarkable in the lower troposphere, with a maximum of O_3 concentration at around 1 km. This peak value at 1 km was also reported by Ding et al. (2008) in the MOZAIC program over Beijing, but not observed in other regions carried out in the last 10 years, e.g. the INTEX-B campaign (Swartzendruber et al., 2008), the ITCT 2K2- PEACE experiments (Parrish et al., 2004), TRACE-P and ACE-ASIA experiments (Price et al., 2004), the PNW2001 field experiments (Snow et al., 2003), the PHOBEA

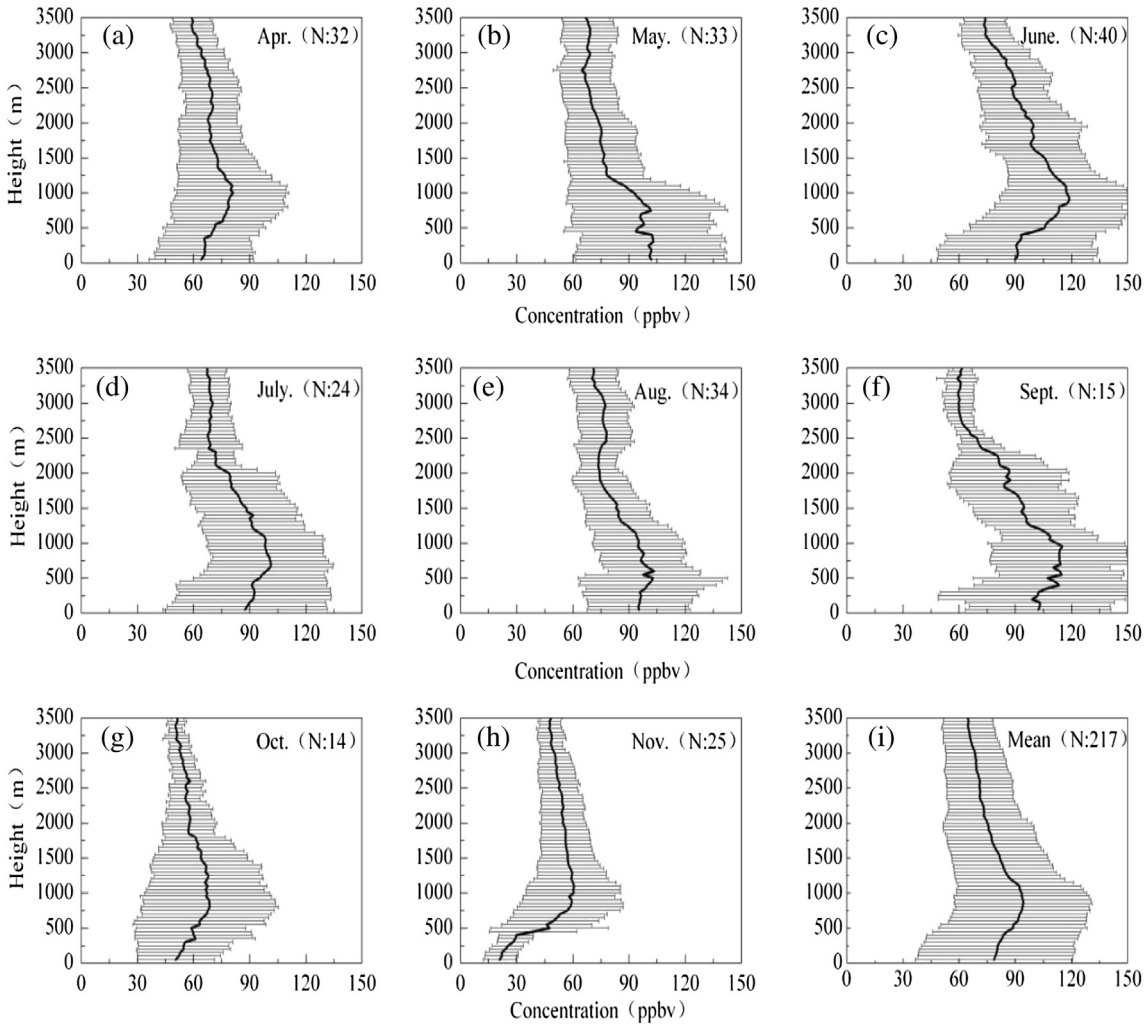

Fig. 2. The O_3 profiles over Beijing from April to November (a–h) and for all data (i). The total number of valid profiles used in statistics is given in the parentheses.

campaigns (Kotchenruther et al., 2001), and the experiments over northeast Pacific (Bertschi et al., 2004; Bertschi and Jaffe, 2005).

Below 1 km, the averaged O_3 concentration had a minimum value at the surface and increased with altitude. For example, the mean ozone concentrations increased from around 80 ppbv below 100 m to about 95 ppbv at the altitude of 900–1000 m (see Fig. 2i). Above 1 km, the O_3 concentration decreased with altitude. For example, the value was around 75 ppbv at 2 km (see Fig. 2i). The mean O_3 concentration at the altitudes of 3–3.6 km was about 66 ppbv, which was similar to the measurements made over the Northwest Pacific (from 45 to 73 ppb) (Swartzendruber et al., 2008), but was slightly higher than the measurement made over the Northeast Pacific (from 40 to 60 ppb) (Bertschi et al., 2004; Bertschi and Jaffe, 2005; Price et al., 2003; Parrish et al., 2004). Our results also suggest that in the lower troposphere (below 2 km), the measured O_3 concentrations were much higher than measurements made over the Northwest and Northeast Pacific, indicating that the heavy atmospheric pollutants emitted in the NCP region had important effects on a regional photochemical O_3 formation in this region.

To better understand the diurnal variation of the measured ozone vertical distributions in the lower troposphere, the hourly-averaged ozone profiles were analyzed. Fig. 3 shows the averaged ozone vertical profiles from 9:00–10:00 am to 17:00–18:00 pm from May to September. The result indicates several important diurnal variations of O_3, especially in the lower troposphere. These variations include that: (1) the ozone peak at about 1 km appeared during daytime, but the magnitude of O_3 changed from the morning (9:00–10:00 am) to the evening (17:00–18:00 pm). For example, the peak values were about 90, 100, and 120 ppbv, at 9:00–10:00 am, 11:00–12:00 am, and 14:00–15:00 pm, respectively. (2) The O_3 concentrations at the higher altitude (3.5 km) were relatively constant, with a value of 60 ppbv during daytime, suggesting that either the O_3 transported from the upper troposphere or the influences from the lower troposphere had insignificant effects on the ozone concentrations at 3.5 km. (3) There was a large variability of ozone concentrations below 1 km (the peak ozone level). The surface ozone concentration was very low (30 ppbv) during the morning at 9:00–10:00 am, and the value rapidly increased and reached to a maximum value of 120 ppbv at 15:00–16:00. The surface ozone diurnal variation was consistent with several previous studies in the Beijing area (Tang et al., 2009; Xu et al., 2011).

In order to investigate the processes that controlled the variation of ozone at different altitudes, the vertical distributions of several related chemical parameters were shown in Fig. 4 (including O_3, $NOx = (NO + NO_2)$, NO/NOx, and $Ox = (O_3 + NO_2)$). Fig. 4 shows the vertical profiles in 4 time periods (such as 9:00–10:00 am (P1), 10:00–11:00 am (P2), 12:00–13:00 pm (P3), and 15:00–16:00 pm (P4)). There were several important aspects shown in Fig. 4. (1) Below 0.5 km, the ozone concentrations rapidly increased from P1 to P4. For example, from P1 to P2, the rate of ozone formation was

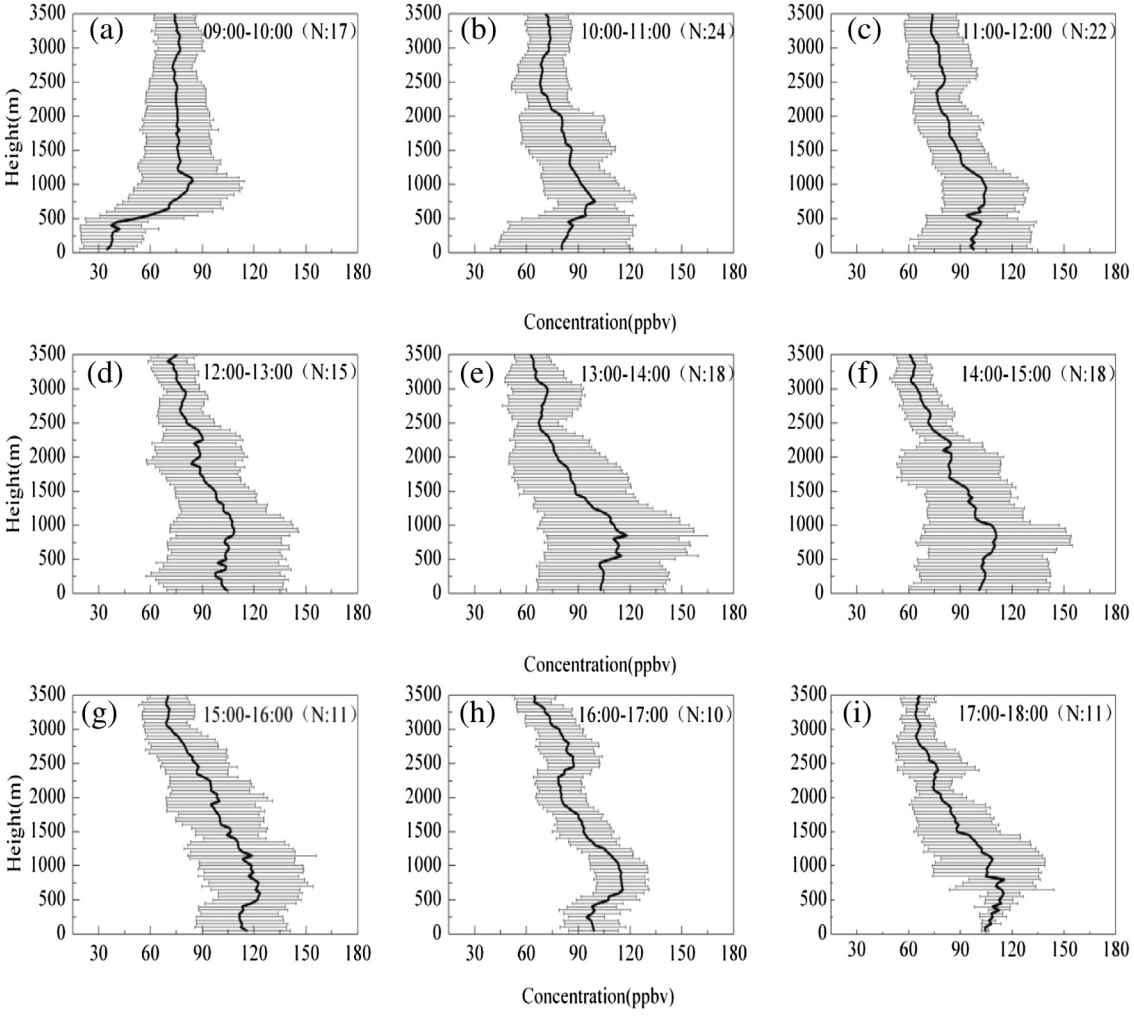

Fig. 3. Diurnal patterns of O_3 profiles over Beijing during May to September (a–i). The total number of valid profiles used in statistics is given in the parentheses.

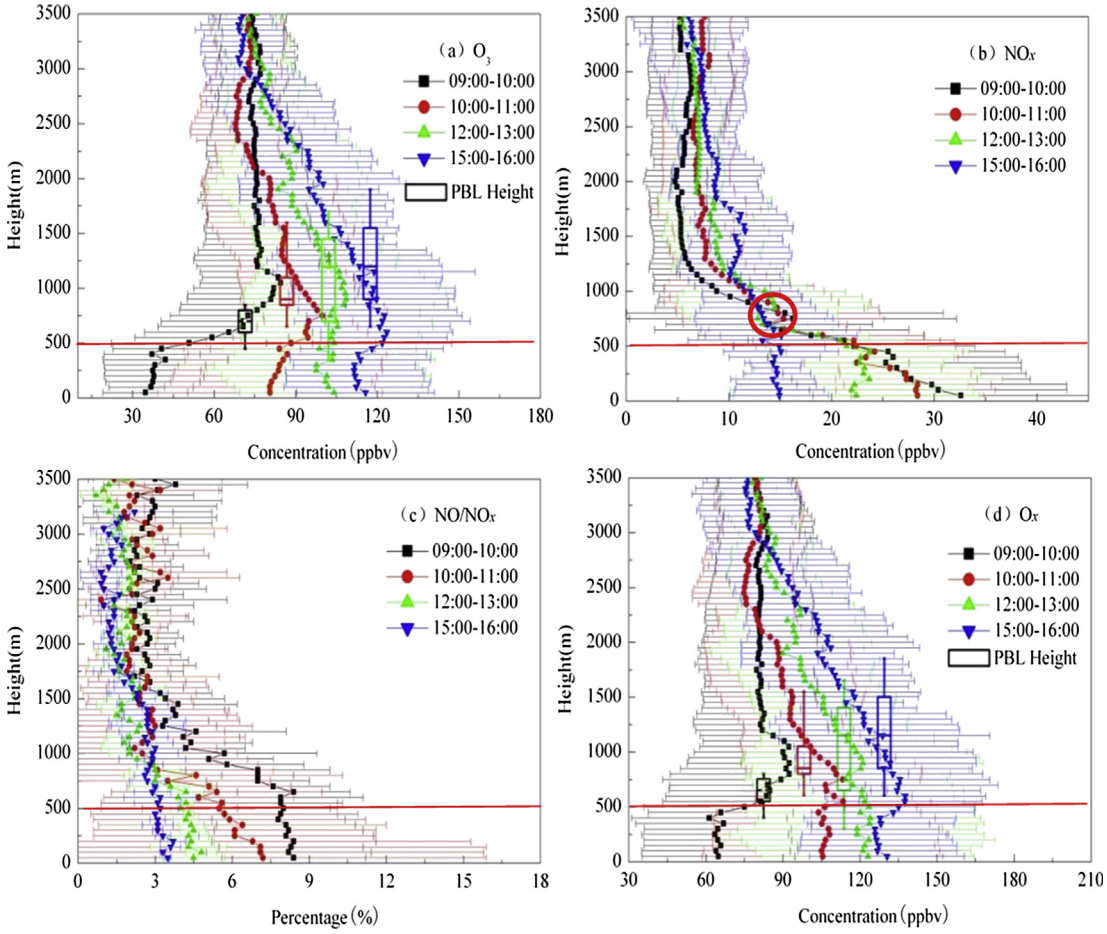

Fig. 4. Diurnal patterns of O_3 profiles over Beijing at 4 periods. The data is the same as Fig. 3. The red circle in b indicates the transition altitude for NOx vertical profiles and their correlation with O_3 concentrations. Under the altitude, O_3 and NOx are anti-correlated, while above the altitude, O_3 and NOx are correlated each other. (For interpretation of the references to color in this figure legend, the reader is referred to the web version of this article.)

about 45 ppb h^{-1} below 0.5 km, with surface concentrations were 32 and 77 ppbv at P1 and P2, respectively. (2) In contrast to the increases in O_3, the NOx concentrations below 0.5 km rapidly decreased. For example, the surface concentrations were 33, 28, 22, and 15 ppbv from P1 to P4, respectively. The time evolution of NO/NOx showed a similar but a larger variation compared with the variation of NOx, especially at the altitude nearby 0.5 km. These anti-correlation between O_3 and NO/NOx suggested that a strong chemical conversion of $O_3 + NO \rightarrow NO_2$. This result is consistent with previous studies that surface O_3 formation was depressed by NOx, and was within the VOC-limited condition (Shao et al., 2009; Lu et al., 2010; Tang et al., 2010). (3) The temporal variation of Ox ($O_3 + NO_2$) was consistent with the variation of O_3, with a smaller magnitude. For example, the changes of the surface concentrations of O_3 were from 32 to 120 ppbv from P1 to P4. In contrast, the changes of the surface concentrations of Ox were from 62 to 130 ppbv. This result indicated that the chemical conversion of $O_3 + NO \rightarrow NO_2$ plays only a partial role for the temporal variation

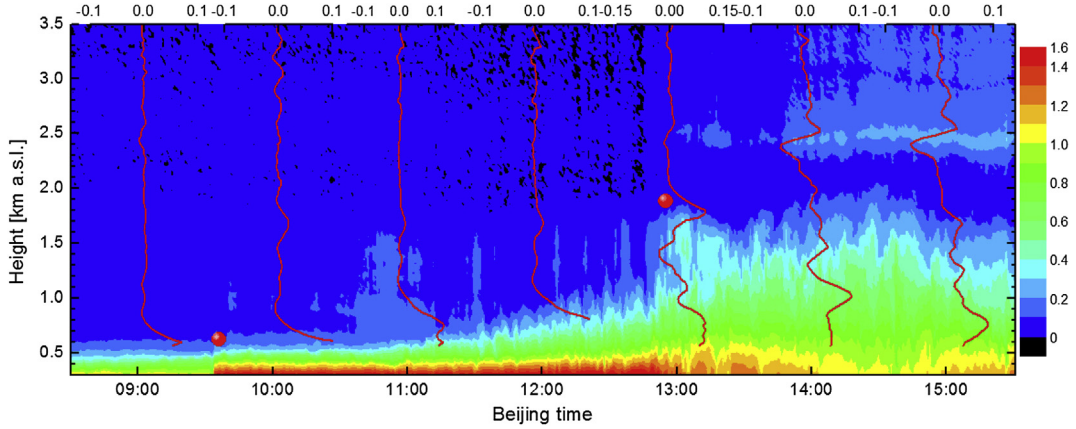

Fig. 5. The development of PBL observed by MPL on Sep/27, 2011, the red point is the height of PBL calculated by aircraft measurement. (For interpretation of the references to color in this figure legend, the reader is referred to the web version of this article.)

of O_3. There are other important processes, which will be further analyzed in the following sections. (4) The PBL (Planetary Boundary Layer) height was estimated in this study by the method that the dew points, which was calculated based on temperature and relative humility, at the height was rapidly deceased (Wilczak et al., 1996; Geng et al., 2009). The height of PBL defined by above method is compared with that defined by Micro Pulse Lidar (MPL-4B, Sigmaspace Co., USA). The calculated PBL heights based on the two methods are consistent (see Fig. 5). Fig. 4 also shows that the PBL heights were 0.6, 0.9, 1.1, and 1.3 km at P1, P2, P3, and P4, respectively. Above the PBL and below 3.0 km, the O_3 and Ox concentrations and variations were very similar, suggested a very small effect of the chemical conversion of $O_3 + NO \rightarrow NO_2$. (5) There was a transition altitude from the negative correlation to the positive correlation between O_3 and NOx. The transition altitude was located at about 1 km (see the red circle in Fig. 4b). As we mentioned before, the negative correlation below 0.5 km showed that the O_3 formation was within the VOC-limited condition. The positive correlation about 1 km suggested that the O_3 formation was within in the NOx-limited condition (i.e., increase in NOx concentrations leads to increase in O_3 concentrations). This result is also consistent with several previous studies that the NOx-limited condition was generally occurred in remote areas from large cities (Madronich, 2006; Tie et al., 2009b).

Fig. 6 shows the vertical distributions of O_3, NOx, Ox, and aerosol concentrations under two different NOx conditions (i.e., high and low NOx conditions). It shows that below 0.5 km, the NOx concentrations were about 15 and 30 ppbv in the low and high NOx conditions, respectively. The corresponding O_3 concentrations were about 87 and 93 ppbv in high and low NOx conditions, respectively. In contrast, the corresponding Ox concentrations were about 125 and 102 ppbv in high and low NOx conditions, respectively. The differences between Ox and O_3 were about 38 and 19 ppbv in high and low NOx conditions, respectively, revealing that a large amount of O_3 was converted to NOx. This process resulted in the lower O_3 concentrations with higher NOx concentrations, and the higher O_3 concentrations with lower NOx concentrations. However, above the 0.5 km, the O_3 and NOx concentrations were correlated to each other, showing a further evidence that the O_3 concentrations were inhibited only occurring in the lower PBL (below 0.5 km), where the O_3 formation was under the VOC-limited condition. About 0.5 km, the O_3 concentrations were higher with the increase of NOx concentrations, showing that the ozone formation was switched to the NOx-limited condition.

3.2. Ozone horizontal distribution over NCP

As indicated in Fig. 1, the flights covered a large horizontal area in NCP. In addition to the vertical distribution of O_3, the horizontal distribution of O_3 in the lower troposphere (2–3.6 km) is studied. In order to better understand the O_3 formation in the region, the back-trajectory analysis (Draxler and Rolph, 2003) is used in this study.

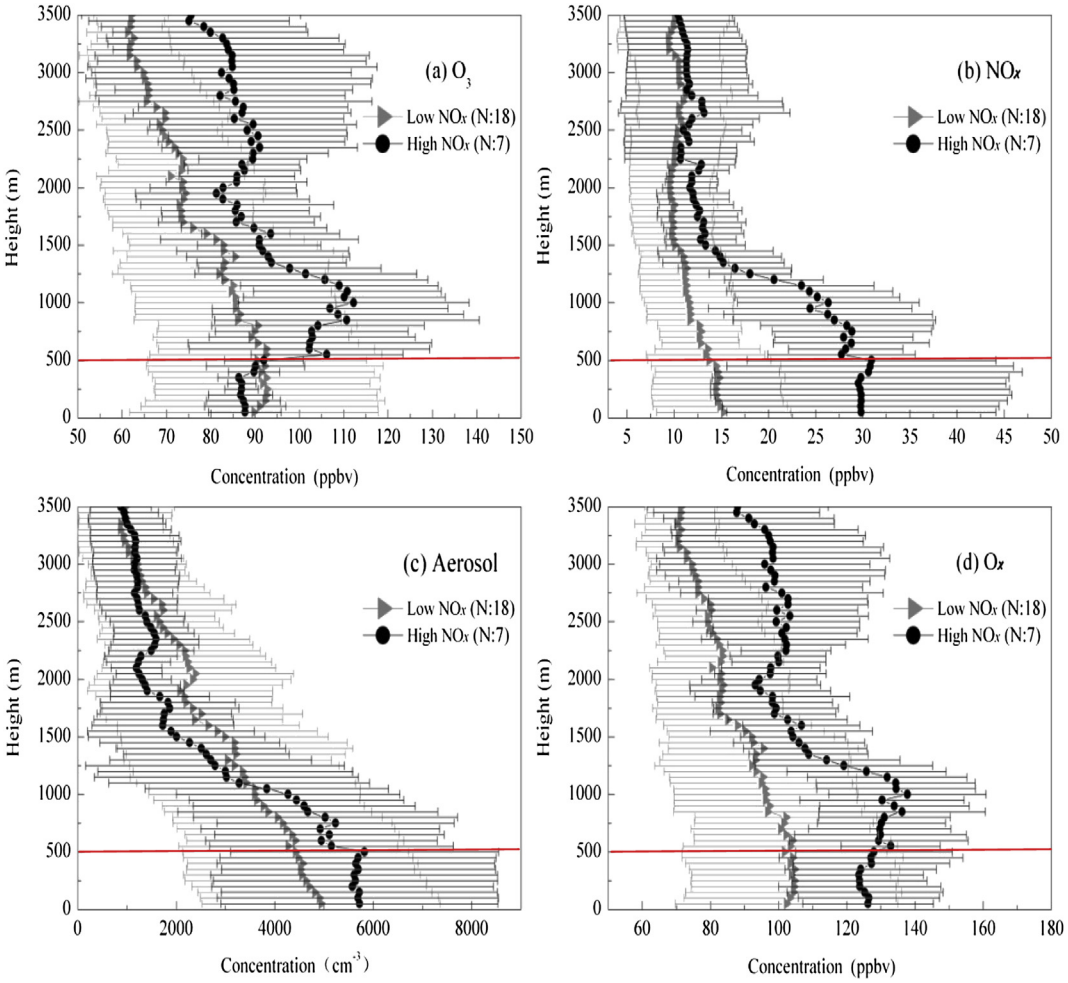

Fig. 6. O_3 profiles under high and low NOx concentration (a), the observations ranging 12:00–18:00 during May to September. The two kinds of NOx profiles are shown in (b), aerosols profiles are shown in (c), and Oz profiles are shown in (d).

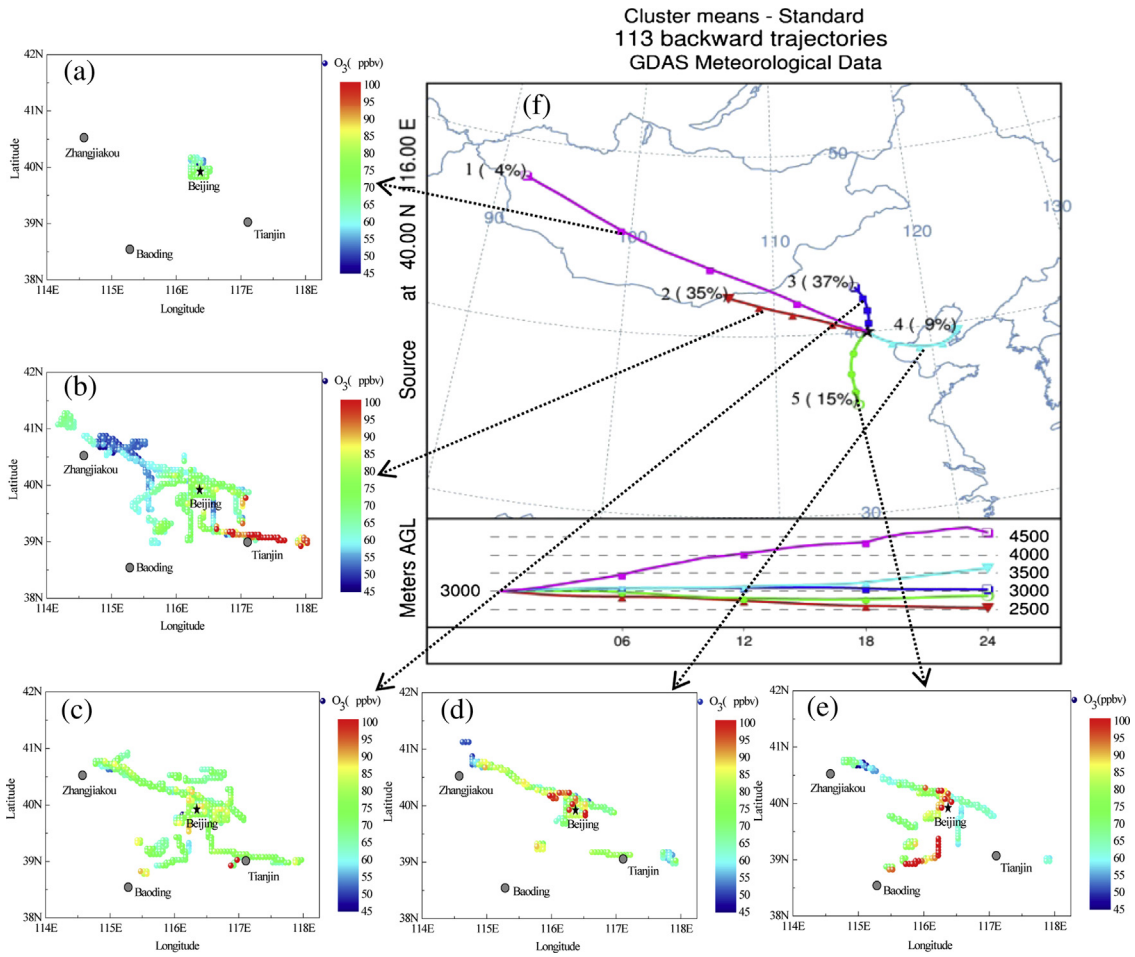

Fig. 7. Clusters of 24 h back-trajectories ending at 3 km over Beijing during May–September during 2007–2010. The O_3 horizontal distributions over NCP in the lower troposphere (2–3.6 km) were classified into 5 categories based on the trajectories: (a) originated from the remote area in the northwest with fast wind speed; (b) from the northwest with slow wind speed; (c) from the remote area in the north; (d) from the polluted regions in the east; (e) from the polluted regions in the south.

Fig. 7 shows one-day back-trajectories at 14:00 LT for all profiles collected from May to September during 2007–2010. The end-points of the trajectories were at 3 km over Shahe Airport (SH). Based on their origins and pathways, the trajectories were classified into five cases, including (1) the air pathway from a long distance of the northwest direction (case-1), (2) the air pathway from a short distance of the northwest direction (case-2), (3) the air pathway from the north direction (case-3), (4) the air pathway from the east direction (case-4), and (5) the air pathway from the south direction (case-5). The detailed pathways for the 5 cases shown in Fig. 7 as indicated by purple, red, blue, light blue and green lines, respectively. (For interpretation of the references to color in this figure, the reader is referred to the web version of this article.)

The horizontal O_3 distributions show in Fig. 7 for the 5 different cases. In the case-1, there was only 4% in all fights, and only small horizontal area was covered. In the case-2, there was 35% in all fights, and O_3 concentrations were low in the upwind region of the mega city (Beijing), and high in the downwind region of Beijing. For example, the O_3 concentration was about 50 ppbv in the upwind region, while it was about 100 ppbv in the downwind region. This result suggests that O_3 was continuously formed in the city plumes, leading to an enhancement in O_3 concentration in the city plumes. This result was also found in another mega city plumes (Mexico City plumes) as shown by Tie et al. (2009b). In the case-4, the wind direction (WD) was reversed compared to the WD in the case-2. As the result, in the upwind region of the city (the downwind region in the case-2), the O_3 concentration was 50–60 ppbv (100 ppbv in the case-2). In contrast, in the downwind region of the city (the upwind region in the case-2), the O_3 concentration was 80–100 ppbv (50 ppbv in the case-2). This result further suggests that O_3 concentration was enhanced in the downwind of the city plumes.

4. Summaries

In this study, the vertical and horizontal distributions of ozone over the NCP region were analyzed based on aircraft measurements during 2007–2010. The results are summarized as follows.

(1) Ozone over Beijing shows different vertical distributions to other observations carried out over the northeast Pacific and Europe. There was a peak of ozone concentrations appeared at around 1 km. Above this altitude, ozone concentration decrease slowly with height in the lower troposphere.
(2) Below the peak value, O_3 was strongly inhibited by high NOx concentrations. The ozone formation was in the VOC-limited condition, and O_3 and NOx concentrations are strongly anti-correlated. Above the peak value, O_3 formation was in the NOx-limited condition, and O_3 and NOx concentrations are strongly correlated.
(3) The analysis of the horizontal distribution of O_3 shows that O_3 was continuously formed inside the city plumes, leading to the enhancement in O_3 concentration in the city plumes. This

result was consistent with the studies in other large city plumes, such as Mexico City plumes.

Acknowledgments

This research is partially supported by National Natural Science Foundation of China (NSFC) under Grant No. 40905060, 41175007, and 41275168; The National Basic Research Program of China (2011CB403401); The Project of Scientific and Technological New Star of Beijing under Grant No. 2010B029.

References

Akimoto, H., 2003. Global air quality and pollution. Science 302, 1716–1719.
An, J.L., 2006. Ozone production efficiency in Beijing area with high NOx emissions. Acta Scientiae Circumstantiae 26, 652–657.
Benjamin, M.T., Winer, A.M., 1998. Estimating the ozone-forming potential of urban trees and shrubs. Atmospheric Environment 32, 53–68.
Bertschi, I.T., Jaffe, D.A., 2005. Long-range transport of ozone, carbon monoxide, and aerosols to the NE Pacific troposphere during the summer of 2003: observations of smoke plumes from Asian boreal fires. Journal of Geophysical Research 110, D05303. http://dx.doi.org/10.1029/2004JD005135.
Bertschi, I.T., Jaffe, D.A., Jaeglé, L., Price, H.U., Dennison, J.B., 2004. PHOBEA/ITCT 2002 airborne observations of transpacific transport of ozone, CO, volatile organic compounds, and aerosols to the northeast Pacific: impacts of Asian anthropogenic and Siberian boreal fire emissions. Journal of Geophysical Research 109, D23S12. http://dx.doi.org/10.1029/2003JD004328.
Bian, H., Han, S.Q., Tie, X.X., Sun, M.L., Liu, A.X., 2007a. Evidence of impact of aerosols on surface ozone concentration in Tianjin, China. Atmospheric Environment 41, 4672–4681.
Bian, J., Gettelman, A., Chen, H., Pan, L.L., 2007b. Validation of satellite ozone profile retrievals using Beijing ozonesonde data. Journal of Geophysical Research 112, D06305. http://dx.doi.org/10.1029/2006jd007502.
Bojkov, R.D., 1988. Ozone changes at the surface and in the free troposphere, tropospheric ozone. In: Isaksen, I.S.A., Reidel, D. (Eds.), Regional and Global Scale Interactions. Dordrecht, Netherlands, pp. 83–96.
Ding, A.J., Wang, T., Thouret, V., Cammas, J.P., Nédélec, P., 2008. Tropospheric ozone climatology over Beijing: analysis of aircraft data from the MOZAIC program. Atmospheric Chemistry and Physics 8, 1–13.
Draxler, R.R., Rolph, G.D., 2003. HYSPLIT (HYbrid Single-Particle Lagrangian Integrated Trajectory) Model Access via NOAA ARL READY. NOAA Air Resources Laboratory, Silver Spring, MD. Website. http://www.arl.noaa.gov/ready/hysplit4.html.
Duan, J., Tan, J., Yang, L., Wu, S., Hao, J., 2008. Concentration, sources and ozone formation potential of volatile organic compounds (VOCs) during ozone episode in Beijing. Atmospheric Research 88, 25–35.
Geng, F.H., Zhang, Q., Tie, X.X., Huang, M.Y., Deng, Z.Z., Yu, Q., Quan, J.N., Zhao, C.S., 2009. Aircraft measurements of O_3, NOx, CO, VOCs, and SO_2 in the Yangtze River Delta region. Atmospheric Environment 43, 584–593.
Han, S.Q., Bian, H., Tie, X., Xie, Y., Sun, M., Liu, A., 2009. Impact measurements of nocturnal planetary boundary layer on urban air pollutants: from a 250 m tower over Tianjin, China. Journal of Hazardous Materials 162, 264–269.
Hao, J., Wang, L., 2005. Improving urban air quality in China: Beijing case study. Journal of the Air & Waste Management Association 55, 1298–1305.
Hübler, G., Alvarez, R., Daum, P., Dennis, R., Gillani, N., Kleinman, L., Luke, W., Meagher, J., Rider, D., Trainer, M., Valente, R., 1998. An overview of the airborne activities during the Southern Oxidants Study (SOS) 1995 Nashville/Middle Tennessee Ozone Study. Journal of Geophysical Research 103 (D17), 22245–22259. http://dx.doi.org/10.1029/98JD01638.
Kotchenruther, R.A., Jaffe, D.A., Jaeglé, L., 2001. Ozone photochemistry and the role of peroxyacetyl nitrate in the springtime northeastern Pacific troposphere: results from the Photochemical Ozone Budget of the Eastern North Pacific Atmosphere (PHOBEA) campaign. Journal of Geophysical Research 106, 28731–28742.
Lu, K.D., Zhang, Y.H., Su, H., Brauers, T., Chou, C.C., Hofzumahaus, A., Liu, S.C., Kita, K., Kondo, Y., Shao, M., Wahner, A., Wang, J.L., Wang, X.S., Zhu, T., 2010. Oxidant ($O_3 + NO_2$) production processes and formation regimes in Beijing. Journal of Geophysical Research 115, D07303. http://dx.doi.org/10.1029/2009JD012714.
Madronich, S., 2006. Chemical evolution of gaseous air pollutants downwind of tropical megacities: Mexico City case study. Atmospheric Environment 40, 6012–6018.
Mcnider, R.T., Norris, W.B., Casey, D.M., Pleim, J.E., Roselle, S.J., Lapenta, W.M., 1998. Assimilation of satellite data in regional air quality models. In: Gryning, S.E., Chaumerliac, N. (Eds.), 1998. Air Pollution Modeling and Its Application, XII. NATO/CCMS, Plenum Press, New York, USA, pp. 25–35.
Ohara, T., Akimoto, H., Kurokawa, J., Horii, N., Yamaji, K., Yan, X., Hayasaka, T., 2007. An Asian emission inventory of anthropogenic emission sources for the period 1980-2020. Atmospheric Chemistry and Physics 7, 4419–4444.
Parrish, D.D., Kondo, Y., Cooper, O.R., Brock, C.A., Jaffe, D.A., Trainer, M., Ogawa, T., Hubler, G., Fehsenfeld, F.C., 2004. Intercontinental Transport and Chemical Transformation 2002 (ITCT 2K2) and Pacific Exploration of Asian Continental Emission (PEACE) experiments: an overview of the 2002 winter and spring intensives. Journal of Geophysical Research 109, D23S01. http://dx.doi.org/10.1029/2004JD004980.
Price, H.U., Jaffe, D., Doskey, P., McKendry, I., Anderson, T., 2003. Vertical profiles of O3, aerosols, CO and NMHCs in the northeast Pacific during the ACE-Asia and TRACE-P experiments. Journal of Geophysical Research 108 (D20), 8799. http://dx.doi.org/10.1029/2002JD002930.
Price, H.U., Jaffe, D.A., Cooper, O.R., Doskey, P.V., 2004. Photochemistry, ozone production, and dilution during long-range transport episodes from Eurasia to the northwest United States. Journal of Geophysical Research 109, D23S13. http://dx.doi.org/10.1029/2003JD004400.
Quan, J.N., Zhang, Q., He, H., Liu, J., Huang, M., Jin, H., 2011. Analysis of the formation of fog and haze in North China Plain (NCP). Atmospheric Chemistry and Physics 11, 8205–8214.
Shao, M., Lu, S., Liu, Y., Xie, X., Chang, C., Huang, S., Chen, Z., 2009. Volatile organic compounds measured in summer in Beijing and their role in ground-level ozone formation. Journal of Geophysical Research 114, D00G06. http://dx.doi.org/10.1029/2008JD010863.
Shao, M., Tang, X.Y., Zhang, Y.H., Li, W.J., 2006. City clusters in China: air and surface water pollution. Frontiers in Ecology and the Environment 4, 353–361.
Sillman, S., 1995. The use of NOy, H_2O_2, and HNO_3 as indicators for ozone–NOx–hydrocarbon sensitivity in urban locations. Journal of Geophysical Research 100 (D7), 14175–14188.
Snow, J.A., Dennison, J.B., Jaffe, D.A., Price, H.U., Vaughan, J.K., Lam, B., 2003. Aircraft and surface observations of air quality in Puget Sound and a comparison to a regional model. Atmospheric Environment 37, 4019–4032.
Swartzendruber, P.C., Chand, D., Jaffe, D.A., Smith, J., Reidmiller, D., Gratz, L., Keeler, J., Strode, S., Jaegle, L., Talbot, R., 2008. Vertical distribution of mercury, CO, ozone, and aerosol scattering coefficient in the Pacific Northwest during the spring 2006 INTEX-B campaign. Journal of Geophysical Research 113, D10305. http://dx.doi.org/10.1029/2007JD009579.
Tang, G., Li, X., Wang, Y., Xin, J., Ren, X., 2009. Surface ozone trend details and interpretations in Beijing, 2001–2006. Atmospheric Chemistry and Physics 9, 8813–8823.
Tang, X., Wang, Z., Zhu, J., Gbaguidi, A.E., Wu, Q.Z., Li, J., Zhu, T., 2010. Sensitivity of ozone to precursor emissions in urban Beijing with a Monte Carlo scheme. Atmospheric Environment 44 (5), 3833–3842.
Tie, X., Cao, J.J., 2009. Aerosol pollution in China: present and future impact on environment. Particuology 7, 426–431.
Tie, X., Geng, F.H., Peng, L., Gao, W., Zhao, C.S., 2009a. Measurement and modeling of O_3 variability in Shanghai, China: application of the WRF-Chem model. Atmospheric Environment 43, 4289–4302.
Tie, X., Madronich, S., Li, G.H., Ying, Z.M., Weinheimer, A., Apel, E., Campos, T., 2009b. Simulation of Mexico City plumes during the MIRAGE-Mex field campaign using the WRF-Chem model. Atmospheric Chemistry and Physics 9, 4621–4638.
Tie, X., Madronich, S., Walters, S., Edwards, D.P., Ginoux, P., Mahowald, N., Zhang, R.Y., Lou, C., Brasseur, G., 2005. Assessment of the global impact of aerosols on tropospheric oxidants. Journal of Geophysical Research 110, D03204. http://dx.doi.org/10.1029/2004JD005359.
Wang, T., Ding, A.J., Gao, J., Wu, W.S., 2006. Strong ozone production in urban plumes from Beijing, China. Geophysical Research Letters 33, L21806. http://dx.doi.org/10.1029/2006GL027689.
Wang, Y., Hao, J., McElroy, M.B., Munger, J.W., Ma, H., Chen, D., Nielsen, C.P., 2009. Ozone air quality during the 2008 Beijing Olympics: effectiveness of emission restrictions. Atmospheric Chemistry and Physics 9, 5237–5251.
Wang, Y., Konopka, P., Liu, Y., Chen, H., Müller, R., Plöger, F., Riese, M., Cai, Z., Lu, D., 2012. Tropospheric ozone trend over Beijing from 2002–2010: ozonesonde measurements and modeling analysis. Atmospheric Chemistry and Physics 12, 8389–8399. http://dx.doi.org/10.5194/acp-12-8389-2012.
Warneck, P., 1988. Chemistry of the Natural Atmosphere. Academic Press, San Diego, pp. 1–757.
Wilczak, J.M., Gossard, E.E., Neff, W.D., Eberhard, W.L., 1996. Ground-based remote sensing of the atmospheric boundary layer: 25 years of progress. In: Garratt, J.R., Taylor, P.A. (Eds.). Boundary-Layer Meteorology, Dordrecht, Boston, pp. 1970–1995.
Xu, J., Ma, J.Z., Zhang, X.L., Xu, X.B., Xu, X.F., Lin, W.L., Wang, Y., Meng, W., Ma, Z.Q., 2011. Measurements of ozone and its precursors in Beijing during summertime: impact of urban plumes on ozone pollution in downwind rural areas. Atmospheric Chemistry and Physics Discussion 11, 17337–17373.
Yang, F., Tan, J., Zhao, Q., Du, Z., He, K., Ma, Y., Duan, F., Chen, G., Zhao, Q., 2011. Characteristics of PM2.5 speciation in representative megacities and across China. Atmospheric Chemistry and Physics 11, 5207–5219.
Zhang, Q., Streets, D.G., He, K., Wang, Y.X., Richter, A., Burrows, J.P., Uno, I., Jang, C.J., Chen, D., Yao, Z., Lei, Y., 2007. NOx emission trends for China, 1995–2004: the view from the ground and the view from space. Journal of Geophysical Research 112, D22306. http://dx.doi.org/10.1029/2007JD008684.